



Tectonics

RESEARCH ARTICLE

10.1002/2014TC003612

Key Points:

- The South Atlantic shows fast spreading rate changes
- They can be explained by temporal changes of pressure-driven asthenospheric flux
- This implies a correlation of horizontal and vertical motions

Correspondence to:

L. Colli,
lorenzo.colli@geophysik.uni-muenchen.de

Citation:

Colli, L., I. Stotz, H.-P. Bunge, M. Smethurst, S. Clark, G. Iaffaldano, A. Tassara, F. Guillocheau, and M. C. Bianchi (2014), Rapid South Atlantic spreading changes and coeval vertical motion in surrounding continents: Evidence for temporal changes of pressure-driven upper mantle flow, *Tectonics*, 32, 1304–1321, doi:10.1002/2014TC003612.

Received 17 APR 2014

Accepted 9 JUN 2014

Accepted article online 18 JUN 2014

Published online 8 JUL 2014

Rapid South Atlantic spreading changes and coeval vertical motion in surrounding continents: Evidence for temporal changes of pressure-driven upper mantle flow

L. Colli¹, I. Stotz^{1,2,3}, H.-P. Bunge¹, M. Smethurst^{4,5}, S. Clark⁵, G. Iaffaldano³, A. Tassara², F. Guillocheau⁶, and M. C. Bianchi¹

¹Department of Earth and Environmental Sciences, Ludwig Maximilian University, Munich, Germany, ²Department of Earth Sciences, Universidad de Concepción, Concepción, Chile, ³Research School of Earth Sciences, Australian National University, Canberra, ACT, Australia, ⁴Avalonia Geophysics, University of Exeter, Exeter, UK, ⁵Computational Geoscience Department, Simula Research Laboratory, Fornebu, Norway, ⁶UMR CNRS 6118 Géosciences Rennes, Université de Rennes 1, Rennes, France

Abstract The South Atlantic region displays (1) a topographic gradient across the basin, with Africa elevated relative to South America, (2) a bimodal spreading history with fast spreading rates in Late Cretaceous and Eo-Oligocene, and (3) episodic regional uplift events in the adjacent continents concentrated in Late Cretaceous and Oligocene. Here we show that these observations can be linked by dynamic processes within Earth's mantle, through temporal changes in asthenosphere flow beneath the region. The topographic gradient implies westward, pressure-driven mantle flow beneath the basin, while the rapid spreading rate changes, on order 10 million years, require significant decoupling of regional plate motion from the large-scale mantle buoyancy distribution through a mechanically weak asthenosphere. Andean topographic growth in late Miocene can explain the most recent South Atlantic spreading velocity reduction, arising from increased plate boundary forcing associated with the newly elevated topography. But this mechanism is unlikely to explain the Late Cretaceous/Tertiary spreading variations, as changes in Andean paleoelevation at the time are small. We propose an unsteady pressure-driven flow component in the asthenosphere beneath the South Atlantic region to explain the Late Cretaceous/Tertiary spreading rate variations. Temporal changes in mantle flow due to temporal changes in regional mantle pressure gradients imply a correlation of horizontal and vertical motions: we find that this prediction from our models agrees with geologic and geophysical observations of the South Atlantic region, including episodes of passive margin uplift, regional basin reactivation, and magmatic activity.

1. Introduction

The South Atlantic holds a prominent place in the history of plate tectonics since *Bullard et al.*'s [1965] fit of South America and Africa showed how both continents were once joined. The region preserves an exceptional archive of past plate motion (Figure 1a) so its spreading history is well known [*Cande et al.*, 1988; *Nürnberg and Müller*, 1991].

Figure 1b shows spreading half rates of the South Atlantic by *Müller et al.* [2008] based on marine magnetic anomaly identifications, following the techniques outlined by *Müller et al.* [1997]. The compilation reveals rapid changes over periods of a few million years (Myr). While it is accepted that buoyancy forces associated with subduction of cold, dense lithosphere provide significant driving forces for plate motion [*Lithgow-Bertelloni and Richards*, 1995], the short duration of the South Atlantic spreading rate changes makes it difficult to attribute them to variations of the large-scale mantle buoyancy distribution, which should evolve on longer timescales on the order of 50 to 100 Myr as suggested by mantle circulation modeling [*Bunge et al.*, 1998].

Some South Atlantic spreading rate changes likely reflect temporal variations in plate boundary forcing, in particular along the western margin of South America. The most significant tectonic change there over the past 25 Myr is the growth of the high Andes, especially the rise of the Altiplano and Puna Plateaus some 10 Myr ago [*Charrier*, 2007; *Garzzone et al.*, 2006; *Oncken et al.*, 2006]. Estimated tectonic forces associated with the current Andean topography amount to $\approx 8 \times 10^{12}$ N/m on average, comparable to the driving forces

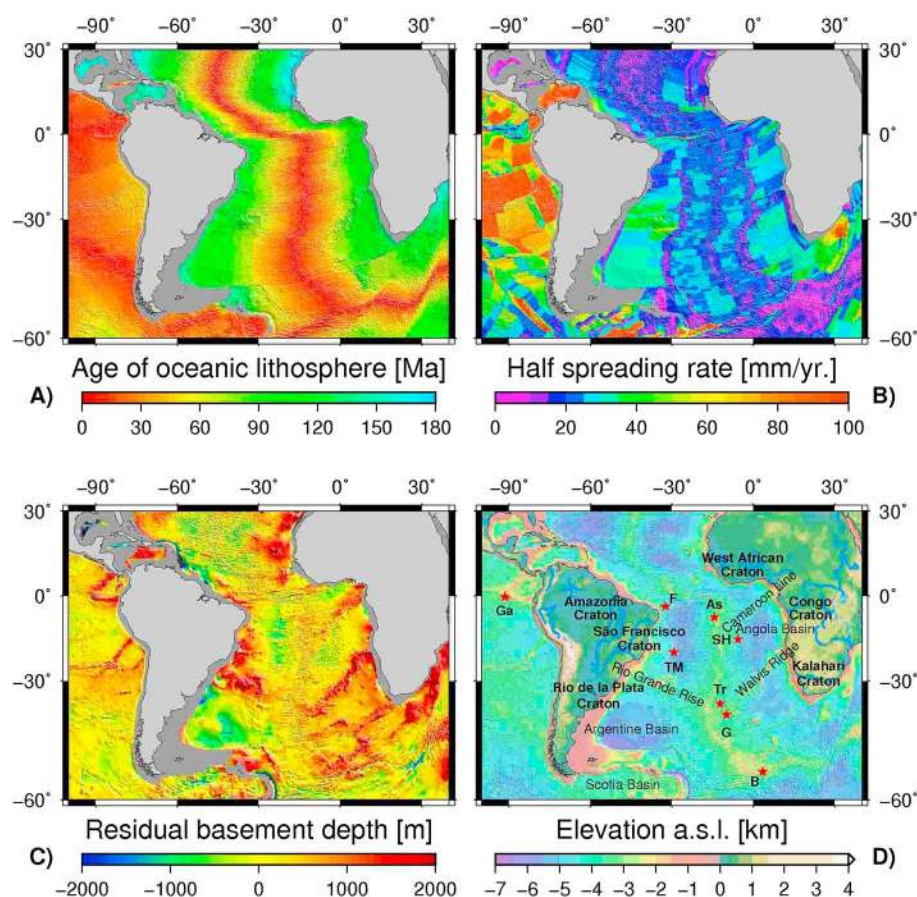


Figure 1. (a) Age-area distribution and (b) half-spreading rates of ocean floor in the South Atlantic region from Müller *et al.* [2008]. (c) Residual basement depth computed by calculating difference between predicted and sediment unloaded basement depth. Predicted basement depth obtained by applying Crosby *et al.*'s [2006] North Pacific thermal boundary layer model to age-area distribution from Müller *et al.* [2008]. (d) Topographic map of the South Atlantic region from the global relief model ETOPO1 [Amante and Eakins, 2009], annotated with major structural elements. Craton names are boldface, while stars denote prominent hot spots (Ga: Galapagos; F: Fernando de Noronha; As: Ascension; SH: Saint Helena; TM: Trinidade and Martim Vaz; Tr: Tristan da Cunha; G: Gough Island; and B: Bouvet Island).

in plate tectonics [Husson and Ricard, 2004; Iaffaldano *et al.*, 2006]. The temporal correlation between recent Andean uplift and plate kinematic changes around South America supports the notion that the load of this newly elevated topography affects plate motions. For instance, the 30% convergence reduction across the Nazca/South America margin in the late Miocene, commonly attributed to growth of the high Andes [e.g., Norabuena *et al.*, 1999], has been linked to a corresponding reduction of South Atlantic spreading rates in a global model of the coupled mantle/lithosphere system [Iaffaldano and Bunge, 2009]. Far-field effects are thus an important influence on South Atlantic spreading. Husson *et al.* [2012], moreover, attributed the most recent South Atlantic spreading rate reduction to the formation of an optimal aspect ratio mantle circulation cell beneath the South Atlantic.

The South Atlantic is also an area of anomalous topography [Winterbourne *et al.*, 2009] with a pronounced bathymetric asymmetry (Figure 1c). The mantle beneath Africa has long been shielded from subduction by the former supercontinent Pangea [Anderson, 1982] and harbors a major low seismic velocity body near the base of the mantle [e.g., Grand, 2002; Ritsema *et al.*, 2011; Romanowicz and Gung, 2002; Simmons *et al.*, 2007]. Much of the low seismic velocity is due to elevated temperature [Davies *et al.*, 2012; Schuberth *et al.*, 2012, 2009a, 2009b]. Thermal upwellings may thus play a prominent role in the South Atlantic, consistent with observations of numerous plume-related volcanic centers (Figure 1d), elevated heat flow in the mobile belts of Southern Africa [Nyblade and Robinson, 1994], and inferences that Africa experienced greater uplift than other continents in the Tertiary [e.g., Bond, 1978; Burke and Gunnell, 2008]. This view is supported by geodynamic studies suggesting that active thermal upwellings in the mantle general circulation account

for as much as 30% (10 TW) of the mantle heat loss [e.g., *Bunge et al.*, 2001; *Bunge*, 2005; *Labrosse*, 2002; *Mittelstaedt and Tackley*, 2006; *Zhong and Leng*, 2006].

Rapid spreading rate changes imply some decoupling of plate motion from the large-scale mantle buoyancy distribution, as noted before, presumably through a mechanically weak asthenosphere [Barrell, 1914]. An asthenosphere was advocated early on in the history of plate tectonics to lubricate plate motion [Chase, 1979] and is supported by rock mechanics arguments [Karato and Wu, 1993; Weertman and Weertman, 1975]. Evidence for an asthenosphere comes from various observations, including global [e.g., Richards and Hager, 1984] and regional [Harig et al., 2010] geoid studies, glacial rebound [e.g., Mitrovica, 1996], oceanic intraplate seismicity [Wiens and Stein, 1985], ocean ridge bathymetry [Buck et al., 2009], seismic anisotropy [e.g., Debayle et al., 2005], and electromagnetic sounding [e.g., Jones, 1982]. Low mechanical strength could arise from weakening associated with partial melt [e.g., Anderson and Sammis, 1970] and/or water [e.g., Karato and Jung, 1998]. A consequence would include the concentration of upper mantle flow into a thin channel of greatly enhanced material mobility. Fluid dynamic studies based on numerical and analytic models [e.g., Bunge et al., 1996; Busse et al., 2006; Tackley, 1996] indicate that high material mobility in the asthenosphere is essential to promote the long-wavelength pattern of mantle flow observed on Earth.

Phipps Morgan and Smith [1992] and *Phipps Morgan et al.* [1995] argued that a plume-fed asthenosphere explains various observations related to ocean bathymetry, heat flow, and mantle geochemistry. A series of papers by *Höink and Lenardic* [2008, 2010] and *Höink et al.* [2011] support the idea that flow in the asthenosphere is caused by lateral pressure gradients (Poiseuille flow) and that the resulting basal shear is the predominant force driving South Atlantic plate motion [Höink et al., 2011]. The concept of asthenosphere flow driven by high- and low-pressure regions relates temporal changes in horizontal motion, i.e., spreading rate changes driven by evolving basal shear forces, explicitly to nonisostatic vertical motion. The latter, known as dynamic topography (see *Braun* [2010] for a review), can be tested with independent data. For instance, *Japsen et al.* [2012a, and references therein] recently drew attention to episodic burial and exhumation of passive continental margins. Such events are well documented along the Brazilian coast [Cogne et al., 2011; Japsen et al., 2012b] and presumably reflect temporal changes in regional dynamic topography.

The focus of this paper is linking horizontal and vertical motion in the South Atlantic region explicitly by evolving upper mantle flow. First, we review the regional tectonics in terms of spreading history, topographic evolution of the Andes, and upper mantle structure constrained from a new tomographic study. We then use simple torque balance models of the South American plate to separate the influence of basal shear forces from plate boundary forces. We demonstrate that the rapid spreading reduction between 80 and 60 Myr followed by renewed and vigorous spreading after 45 Myr is unlikely to result from plate boundary forcing associated with the Andes, as topography along South America's western margin is low at the time. We then turn our attention to Poiseuille flow and show that the current basin-wide dynamic topography gradient may reflect significant pressure-induced upper mantle flow across the South Atlantic region. The magnitude of the Poiseuille flow velocities is comparable to those suggested from basal shear. We test the hypothesis of time-evolving upper mantle flow caused by time-evolving pressure gradients with geologic observations and find that fast spreading periods in the Late Cretaceous and Eocene coincide with regional topographic uplift events in the African and South American continents. We conclude with considerations on rheology and the general style of mantle convection.

2. Tectonic Setting in the South Atlantic Region

2.1. South Atlantic Spreading History

A number of plate motion models are available for the South Atlantic. We compare six models: Earthbyte [Müller et al., 2008], UTIG [Coffin et al., 1998], NGU [Labails et al., 2009; Torsvik et al., 2009], Moulin [Moulin et al., 2010], and two commercial models, A and B. The models differ in the positions of Euler poles, angular velocities, and the locations of plate boundaries, reflecting different interpretations of paleomagnetic and geologic data. Because each model applies its own geologic timescale, we make the models comparable by using a single timescale: *Channell et al.* [1995] from the opening to the M0 anomaly, and *Gradstein et al.* [2004] from M0 to the present. Taking a point presently located in the Salado subplate of South America (57.2°W, 36°S), we calculate the total spreading rate (with respect to Africa) of each of these models. The resulting rates are reported in Figure 2 from 150 Myr to the present.

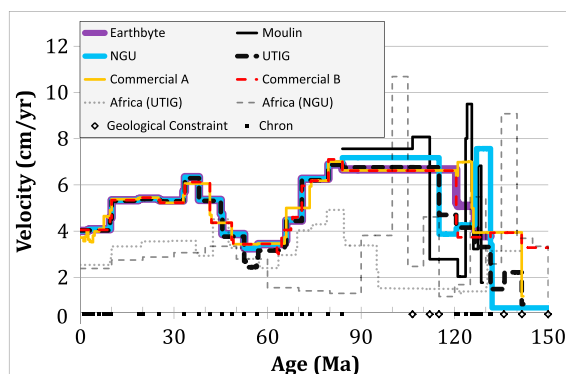


Figure 2. South Atlantic spreading rate for different plate reconstruction models from 150 Myr to the present for a point currently located at 57.2°W, 36°S in a reference frame that keeps Africa fixed. Chrons (squares) and geological constraints dated by particular boundaries (diamonds) used by one or more of the models are shown along the horizontal axis. All models record a spreading rate minimum at around 60 Myr. The curves Africa (NGU) and Africa (UTIG) show the absolute velocities of Africa in a mantle reference frame for an approximately conjugate point in the Orange Basin, at 15°E, 27.5°S.

The curves are similar from C34 (84 Myr) to the present because the rotations are based on similar models. The NGU, Earthbyte, and UTIG models are based on Müller *et al.*'s [1999] reconstruction; Commercial B is based on Cande *et al.* [1988]; and Commercial A is based on a combination of Cande *et al.* [1988] from C4A (8.8 Myr) until the present and Shaw and Cande [1990] from C34 (84 Myr) until C4A. In the early rifting the models vary, although a number of them use Nürnberg and Müller [1991] for the M4 (124.5 Myr) and the M0 (120.6 Myr) anomalies. All models reveal a similar spreading history after around 100 Myr, with a pronounced minimum in the Cretaceous/Tertiary boundary. Spreading is fastest in the Late Cretaceous, drops by a factor of 2 from around 6 to 3 cm/yr between 80 and 70 Myr, stays constant for 10–20 million years before rising back

to almost 6 cm/yr in the middle Eocene, only to decrease again to the current value of about 3.5 cm/yr. Because these rates are reconstructed over intervals of at least 5 Myr, we are confident that the bias of finite-rotation noise [e.g., Iaffaldano *et al.*, 2012] arising from the challenge of precisely identifying the magnetization pattern of the ocean floor and the uncertainty on the geomagnetic polarity timescale is negligible in these models.

It has been proposed [e.g., Silver *et al.*, 1998] that the South Atlantic spreading changes reflect motion of Africa in a mantle reference frame. Thus, Figure 2 also shows the reconstructed absolute motion of Africa according to two different models. The Africa (NGU) curve combines O'Neill *et al.*'s [2005] moving hot spot frame for 100 Myr and younger with Steinberger and Torsvik's [2008] true polar wander frame between 100 Myr and 150 Myr. The Africa (UTIG) curve is based on the fixed hot spot frame of Duncan and Richards [1991] until the middle of their C13–C6 stage (28.5 Myr) and then Müller *et al.*'s [1993] fixed hot spot frame until 130 Myr. While some part of the South Atlantic spreading changes may be ascribed to African absolute motion from C34 to C25 (84 Myr to 56.7 Myr) in the Africa (UTIG) curve, neither the bulk of the spreading variations cannot be explained this way nor can the magnitude of the changes. The spreading rate changes must arise from other forces.

2.2. Topographic Evolution of the Andes

Gansser [1973] divided the Andean chain into a Northern (~12°N to ~5°S), Central (~5°S to ~37°S), and Southern unit (~37°S to ~55°S). The Central unit is characterized by the Altiplano and Puna Plateaus, a magmatic arc (e.g., Western Cordillera) to the west, and a tectonically shortened Eastern Cordillera and foreland to the east [Sempere *et al.*, 2008]. Most models of the orogenic history of the Andes have three main phases [Steinmann *et al.*, 1929]: *Peruvian* during Late Cretaceous, *Incaic* in middle Eocene (or Oligocene, according to Sempere *et al.* [1990]), and *Quechua* since late Miocene. The Northern Central Andes were probably tectonically active during Late Cretaceous [Jaillard, 1994; Sempere *et al.*, 1997]. In latest Cretaceous and early Paleocene, a time also referred to as the KT Orogeny [Charrier, 2007], tectonic activity also took place in the Central Orocline [Charrier, 2007; Cornejo, 2003; Mpodozis *et al.*, 2005] and South Central Andes [Orts and Ramos, 2006; Sempere *et al.*, 1994]. Although no clear evidence exists for Andean paleoelevation in latest Cretaceous and early Paleocene, the scarcity of compressional structures and the small amounts of estimated crustal shortening indicate that elevation presumably was low.

Most studies agree that prominent uplift of the mountain chain started in middle Eocene, reaching a peak in the Oligocene, with a second uplift period in late Miocene [Sempere *et al.*, 1990, 2008]. Middle Eocene and early Oligocene exhumation occurs in the Central Andes [Barnes *et al.*, 2006; Ege *et al.*, 2007; Gillis *et al.*, 2006] with coactivity in the North Central Andes [Hoorn *et al.*, 2010; Jaillard and Soler, 1996; Sebrier *et al.*,

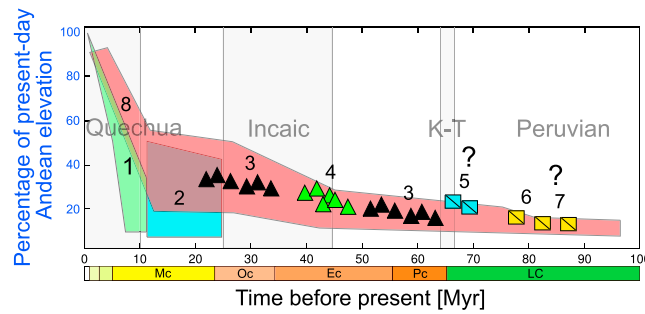


Figure 3. Inferred Andean topographic evolution since Late Cretaceous, plotted relative to today, from a variety of proxies: (1) oxygen isotopes [Garzione et al., 2006; Ghosh et al., 2006], (2) leaf morphology [Gregory-Wodzicki, 2000], (3) apatite fission track (AFT) in the North Central Andes and Central Orocline [Hoorn et al., 2010], (4) AFT in the Central Orocline [Gillis et al., 2006], (5) unconformities in the Central Orocline [Cornejo, 2003], (6) tectonic activity related to uplift in the Central Orocline [Sempere et al., 1997], and (7) tectonic activity related to uplift in the Northern Central Andes [Jaillard, 1994]. Pink region encompasses the average elevation and uncertainties, with question marks signaling times when elevation is poorly constrained but presumably low. Mc, Oc, Ec, Pc, and LC denote Miocene, Oligocene, Eocene, Paleocene, and Late Cretaceous, respectively.

1988]. Significant topographic uplift is inferred since late Miocene from paleosol carbonates [Barke and Lamb, 2006; Ghosh et al., 2006; Schildgen et al., 2007; Thouret et al., 2007] and paleomagnetic data [Rousse et al., 2003]. Gregory-Wodzicki [2000] reached similar conclusions, although leaf morphology studies appear to underestimate paleoelevations [Sempere et al., 2008]. Figure 3 summarizes the tectonic and topographic evolution of the Andes. Notice how the paleoelevation of the mountain chain was likely significantly lower in the Late Cretaceous and Paleocene compared to today, with prominent uplift starting in middle Eocene.

2.3. Regional Upper Mantle Seismic Structure

Upper mantle structure in the South Atlantic region is not well known. Sparsity of seismic stations and the

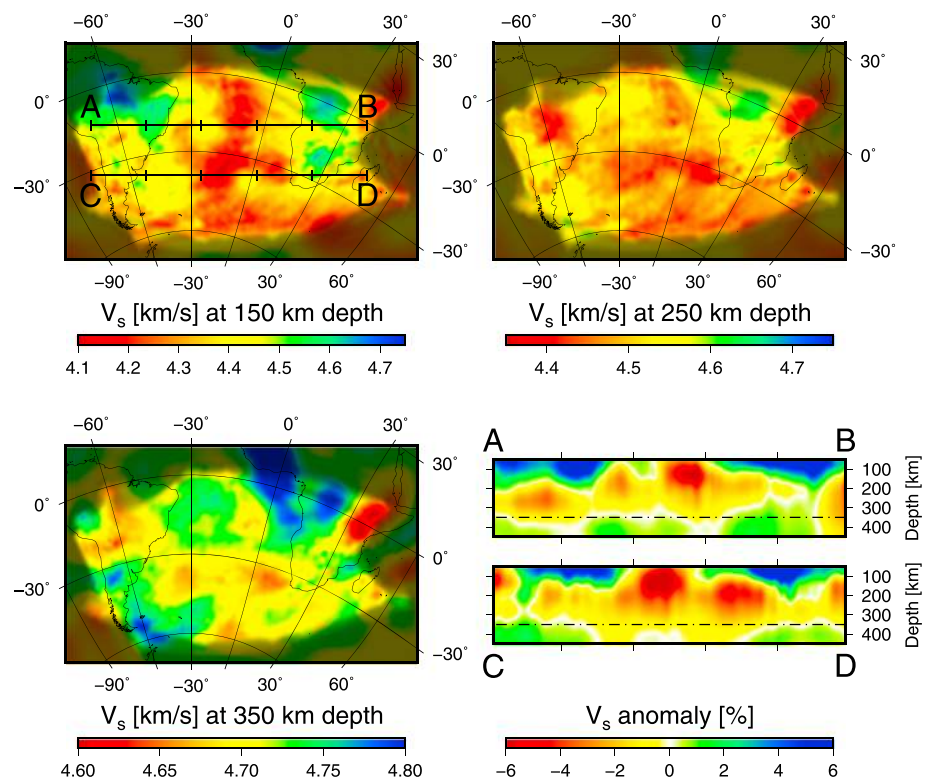


Figure 4. Horizontal slices of upper mantle seismic structure for the South Atlantic region in oblique Mercator projection, together with two vertical transects [Colli et al., 2013]. Shaded regions mark insufficient model resolution. Lines AB and CD on the 150 km depth slice (top left) show location of the two vertical transects (bottom right). The mantle is overall slow, except for fast continental roots, with slow anomalies elongated in a generally east-west direction. The pronounced slow seismic anomalies cease below about 350 km depth, where the structure transitions into a pattern dominated by vertically oriented, columnar slow anomalies embedded in an overall faster mantle.

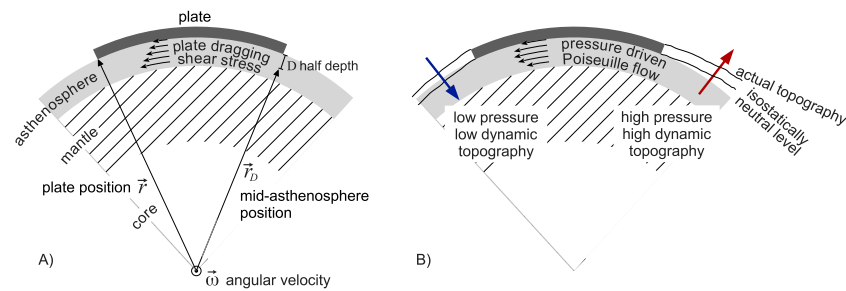


Figure 5. Diagram illustrating geometry and main features of (a) the tectonic force balance model and (b) the fluid dynamic scaling analysis. The tectonic model assumes a rigid plate overlying an isoviscous asthenosphere of constant thickness, allowing us to estimate the excess velocity in the asthenosphere needed to balance all other tectonic forces through basal drag (see equation (2)). The fluid dynamic scaling analysis ascribes the excess velocity explicitly to a pressure-driven Poiseuille flow, whose implications for spatial variations of dynamic topography are shown.

existence of large aseismic areas on the African and South American plates make it difficult to image seismic heterogeneity especially beneath the ocean.

The oceanic upper mantle is imaged primarily by global tomographic studies [e.g., Houser *et al.*, 2008; Kustowski *et al.*, 2008; Panning and Romanowicz, 2006; Ritsema *et al.*, 2011; Shapiro and Ritzwoller, 2002; Simmons *et al.*, 2006]. These reveal overall lower than average seismic velocities, although details differ for scales less than ~ 2000 km [Becker and Boschi, 2002; Dziewonski, 2005]. Some differences may originate from different data sets and model parameterization, whereas others may reflect the approximations associated with raypath tomography [Spetzler *et al.*, 2002; Wang and Dahlen, 1995; Zhou *et al.*, 2005].

Here we take the recent regional tomographic study of Colli *et al.* [2013], based on long-period surface and body waves inverted with a full-waveform methodology, providing a good resolution of the upper South Atlantic mantle above 400 km depth. Figure 4 shows horizontal slices through the model and two vertical transects. While the mantle in the South Atlantic region is overall slow, except for fast continental roots, the vertical transects show a pattern of pronounced slow seismic anomalies that is quite shallow and ceases below about 350 km. At greater depth the horizontal slow seismic velocity anomalies give way to vertically oriented, columnar slow seismic anomalies embedded in a faster mantle. Similar slow velocity anomalies, elongated in the general direction of plate motion, were reported recently for other oceanic basins [e.g., French *et al.*, 2013; Lekić and Romanowicz, 2011; Rickers *et al.*, 2013].

3. Torque Balance Estimates for the South American Plate

To explore possible causes of the velocity changes in the South Atlantic spreading history, we estimate the tectonic torques acting upon the South American plate from 1-D torque balance models. Such models have a long history [e.g., Forsyth and Uyeda, 1975] and, although highly simplified and conceptual, have the advantage of keeping the various tectonic torques separate and identifiable. Combined with geological and geophysical considerations, this allows us to disregard those forces that, due to their known slow temporal variation, cannot produce the rapid variations in the spreading rate.

We start by separating the total tectonic torque into net pull (\vec{M}_{sp}) exerted on the trailing plate by lithospheric slabs descending into Earth's mantle, gravitational spreading of large topographic features such as continental plateaus (\vec{M}_{mb}) or thermally subsiding oceanic lithosphere (the latter is known as the *ridge push*, which we denote here as \vec{M}_{rp}), viscous stresses associated with basal drag at the base of the lithosphere (\vec{M}_{bd}) arising from mantle convective motions, and frictional torques along the uppermost, brittle zone of plate margins (\vec{M}_{fr}). Basal drag is often assumed to resist plate motions but may as well drive it. No slab is currently attached to South America or has one been since at least the Mesozoic. The motion of South America is then governed by a balance of the following torques:

$$\vec{M}_{fr} + \vec{M}_{mb} + \vec{M}_{rp} + \vec{M}_{bd} = 0. \quad (1)$$

For present-day conditions, each torque may be estimated with reasonable confidence. Molnar and Stock [2009] quantified gravitational spreading of continental plateaus through energy balance arguments.

Table 1. Flow Velocities at Present Day Within the Asthenosphere Beneath the South American Plate Required by the Torque Balance (See Equation (2)) to Sustain Current Andean Elevation for a Variety of Asthenosphere Thickness and Viscosity Combinations^a

Viscosity	Asthenosphere Channel Thickness				
	100 km	200 km	300 km	400 km	500 km
1×10^{18} Pa s	81.2	154.5	226.7	298.5	370.0
5×10^{18} Pa s	17.5	32.2	46.6	61.0	75.3
1×10^{19} Pa s	9.5	16.9	24.1	31.3	38.4
5×10^{19} Pa s	3.2	4.6	6.1	7.5	8.9
1×10^{20} Pa s	2.4	3.1	3.8	4.5	5.3

^aUnits are cm/yr. Flow velocities are reported for the middepth of the asthenosphere, where the Poiseuille flow component is close to maximum. Preferred thickness-viscosity combination is marked in boldface.

Ridge push is estimated from the isostatic balance of oceanic lithosphere [e.g., Fowler, 1990], while torques associated with frictional sliding along western South America may be assessed from the effective friction coefficient along plate margins, which we assume depends primarily on the sediment intake [e.g., Iaffaldano, 2012] and tends to be low relative to a Byerlee estimate [Carena and Moder, 2009; Iaffaldano et al., 2006; Suppe, 2007]. For basal drag from a Newtonian viscous mantle, we write

$$\vec{M}_{bd} = \int_A \left[\vec{r} \times \mu \frac{d\vec{v}}{dr} \right] dA, \quad (2)$$

where the shear stress on the plate base at position \vec{r} is the product of viscosity (μ) and radial velocity gradient, while A is the basal plate area (see Figure 5a for a sketch of model geometry). To clarify the dependence of the numerical results on model parameters, one may approximate the velocity gradient by assuming a linear increase with depth:

$$\vec{M}_{bd} = \int_A \left[\vec{r} \times \mu_D \frac{\vec{v}_a - \vec{v}_p}{D} \right] dA,$$

where \vec{v}_p is the plate velocity, \vec{v}_a is the flow at depth D within the asthenosphere, which we choose to be the midpoint of the asthenospheric layer, and μ_D is the viscosity averaged from the plate base to depth D . Plates can be approximated as rigid bodies whose motions are described by Euler vectors ($\vec{\omega}_p$). The mantle, in contrast, behaves as a viscous fluid. For clarity we assume nevertheless that asthenosphere flow beneath the South Atlantic realm may be approximated crudely using a time-dependent Euler vector ($\vec{\omega}_a$), with $|\vec{r}_D| = (r - D)$, and obtain

$$\begin{aligned} \vec{M}_{bd} &= \int_A \left[\vec{r} \times \mu_D \frac{(\vec{\omega}_a \times \vec{r}_D) - (\vec{\omega}_p \times \vec{r})}{D} \right] dA \\ &= \int_A \left[\vec{r} \times \mu_D \frac{\vec{\omega}_a \times \vec{r}_D}{D} \right] dA - \int_A \left[\vec{r} \times \mu_D \frac{\vec{\omega}_p \times \vec{r}}{D} \right] dA. \end{aligned} \quad (3)$$

Equation (3) shows that this torque has two parts [Höink et al., 2011]. The first integral is the Poiseuille component of mantle flow, while the second provides an estimate of the Couette counterpart associated with plate motions. The unknowns are $\vec{\omega}_a$, D , and μ_D , whereas the area and Euler vector of the plate may be inferred from the geologic record. Substituting (3) into (1) allows us to solve for $\vec{\omega}_a$ and the associated basal drag M_{bd} needed to balance the current Andean elevation. We consider a number of combinations of D and μ_D in Table 1, showing that mantle flow velocities scale with D/μ_D , as expected.

The South Atlantic spreading record allows us to extend our scaling to earlier times. To this end, we assume steady mantle flow, constant frictional forces, and constant ridge push since the latest Mesozoic. These assumptions, although simplifying, are motivated by the fact that all these three force components are expected to vary smoothly and over longer timescales with respect to the observed spreading rate variations. For instance, mantle flow changes significantly over time intervals of the order of the transit time (100 Myr), which is the time necessary to cross the mantle by advection. Ridge push increases linearly with plate age for a half-space cooling model or to an asymptote assuming a plate cooling model. In this case, equation (1) allows us to relate the South American velocity record to temporal variations in the torques associated with the Andes. In other words, we equate spreading changes ($\Delta\vec{\omega}_p$) exclusively with changes in the orogenic load

$$\Delta\vec{M}_{mb} = \int_A \left[\vec{r} \times \mu_D \frac{\Delta\vec{\omega}_p \times \vec{r}}{D} \right] dA. \quad (4)$$

Our scaling makes an explicit prediction—relative to today—for the evolution of Andean elevation.

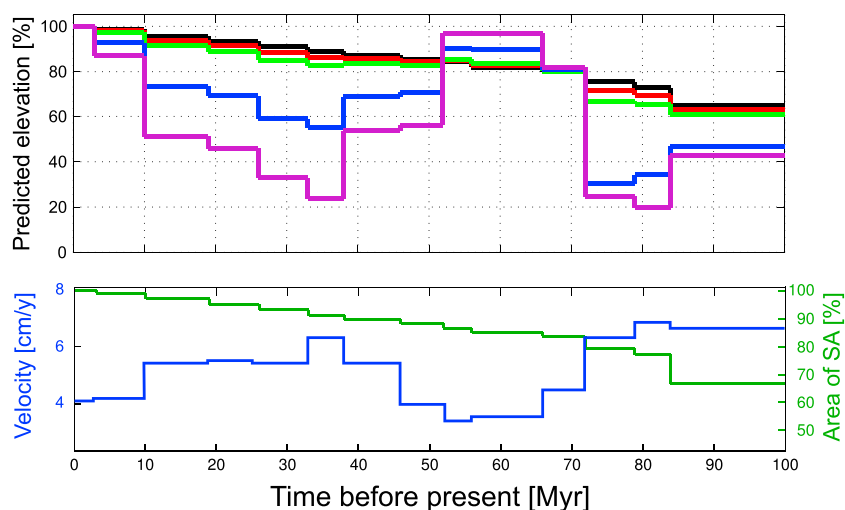


Figure 6. (top) Predicted evolution of Andean paleoelevation, in percent of present elevation, required to balance temporal variations in South American plate velocity and size since mid-Cretaceous, for a variety of asthenosphere viscosities. Black, red, green, blue, and purple lines correspond to 1×10^{18} Pa s, 5×10^{18} Pa s, 1×10^{19} Pa s, 5×10^{19} Pa s, and 1×10^{20} Pa s, respectively. (bottom) Reconstructed South American plate area (green curve) and spreading rate (blue curve) according to the Earthbyte model. Note that for low viscosities (green, black, and red curves in Figure 6, top), estimated Andean paleoelevation scales with South American plate area, while it scales inversely with the plate velocity for higher viscosities (blue and purple curves). Comparison with Figure 3 shows that high- and low-viscosity end-members are both incompatible with geologic inferences of Andean topographic evolution.

Figure 6 shows our results for a range of mantle viscosities, assuming a 300 km thick asthenosphere channel, as suggested by our tomographic results (Figure 4). Two end-member regimes are apparent. For low asthenosphere viscosities and correspondingly high flow velocities, the plate velocity changes imply minor changes in the effective basal drag. In other words, the recorded spreading changes are small relative to the assumed upper mantle flow velocities (Table 1). In this case, inferred elevation changes scale directly with the plate size (compare black, red, and green curves with plate size in Figure 3), and we predict that the mountain chain would remain high throughout the Cenozoic to balance the effective torques. Assuming larger asthenosphere viscosities and correspondingly lower mantle flow velocities instead, the recorded South American plate motion history implies significant basal drag changes. Correspondingly, large temporal changes in the height of the Andes are required to balance the evolving shear stress. Inferred Andean elevation in this case scales inversely with the spreading history (compare blue and purple curves to Figure 2).

Both end-members are incompatible with the inferred topographic evolution of the Andes (Figure 3), and we find that the early Tertiary South Atlantic spreading variations cannot be attributed to Andean elevation changes. All combinations of model parameters yield estimates for the average Andean elevation in Late Cretaceous and early Paleocene that are too large (50% or higher from ~ 70 to ~ 40 Myr) compared to geologic constraints. Hence, we deduce that our assumptions of steady Poiseuille flow and steady basal drag are unrealistic. It seems logical then to consider an unsteady flow component that evolves on shorter timescales than the pattern of large-scale mantle circulation driven by temporal pressure variations in the asthenosphere beneath the South Atlantic region.

4. Asthenosphere Flow

Rapid spreading rate changes in the South Atlantic imply decoupling of plate motion from the large-scale mantle buoyancy distribution, presumably through a mechanically “weak” (i.e., low viscosity) asthenosphere. Postglacial rebound (PGR) provides one of our most direct constraints on mantle rheology. Since the pioneering work of *Haskell* [1935], where he calculated the viscosity of the upper part of the mantle to be $\sim 10^{21}$ Pa s (known as Haskell constraint), PGR studies focused on resolving the radial mantle viscosity distribution. A general consensus exists that the average viscosity of the sublithospheric upper mantle is smaller than that of the deeper mantle, even if the amount of viscosity contrast and the thickness of the

Table 2. Calculated Poiseuille Mantle Flow Velocities in cm/yr in an Asthenosphere Channel Beneath the South Atlantic Region for a Pressure Gradient of 300 Bar Across the Basin and a Variety of Channel Widths and Asthenosphere Viscosities (See Text)^a

Viscosity	Asthenosphere Channel Thickness				
	100 km	200 km	300 km	400 km	500 km
1×10^{18} Pa s	16.9	67.6	152.0	270.3	422.3
5×10^{18} Pa s	3.4	13.5	30.4	54.1	84.5
1×10^{19} Pa s	1.7	6.7	15.2	27.0	42.2
5×10^{19} Pa s	0.3	1.3	3.0	5.4	8.4
1×10^{20} Pa s	0.2	0.7	1.5	2.7	4.2

^aFlow velocities are reported for the middepth of the asthenosphere, where the Poiseuille flow component is close to maximum. Preferred thickness-viscosity combination is marked in boldface.

ity reduction. The trade-off exists also in modeling the geoid [Schaber et al., 2009] and arises because the decay time τ varies linearly with viscosity μ and inversely with h^3 [Cathles, 1975], in the limit of a small-layer thickness h relative to the loading wavelength:

$$\tau \propto \frac{\mu}{h^3}.$$

Equivalently, in the long-wavelength limit, the load may be accommodated by horizontal (Poiseuille) flow in the low-viscosity layer. The significant parameter here is the volumetric flow rate [Davies, 1999], dependent on μ and h^3 , where P' is a pressure gradient:

$$Q = \frac{P'h^3}{12\mu},$$

Assuming the low seismic velocity layer imaged in Figure 4 indicates a low-viscosity channel, a channel thickness of about 300 km, and the Haskell constraint yields an effective viscosity of $\sim 10^{19}$ Pa s.

In addition to spreading rate changes, the South Atlantic sustains a topography gradient which is likely of dynamic origin (see Figures 1c and 5b). On the eastern side, elevated topography, termed the *African superswell* [Nyblade and Robinson, 1994], consists of uplifted portions of the African continent and areas of abnormally high bathymetry in the southeastern Atlantic, whereas much of the southwestern Atlantic, especially in the Argentine Basin, is abnormally deep. The basin-wide dynamic topography gradient in excess of ~ 1 km implies lateral pressure differences in excess of ~ 300 bar. Significant pressure-driven (Poiseuille) flow is thus expected in the sublithospheric mantle. Supporting evidence for westward fluxing upper mantle comes from seismically imaged flow-like structures [French et al., 2013] and geodynamic investigations of upper mantle flow around the southern tip of South America [Nerlich et al., 2013]. The magnitude of Poiseuille flow is readily calculated

$$V_m = \frac{h^2 \Delta P}{8\eta \Delta x}, \tag{5}$$

where ΔP is the pressure difference and Δx is the length scale across the basin. The computed flow velocities depend on the assumed viscosity (η) and thickness (h) of the channel (Table 2). A channel thickness of 300 km, together with an assumed asthenosphere viscosity of 10^{19} Pa s yields good agreement between velocities predicted from pressure-driven flow and those required to sustain the current Andean load through basal shear (Table 1).

5. Spreading Rate Changes and Coeval Epeirogenic Motion in the South Atlantic Region

It seems likely that temporal variations in upper mantle flow associated with temporal changes of pressure gradients should be linked to changes in dynamic topography. This linkage between changes in horizontal and vertical motion can be tested with geologic data. As noted earlier, the South Atlantic has a bimodal spreading history (Figure 2) with high spreading rates in Late Cretaceous and Eo-Oligocene. Thus, it is reasonable to explore the consequences for regional dynamic topography from attributing these changes to unsteady upper mantle flow induced by temporal variations of the pressure gradients in the asthenosphere.

low-viscosity layer remain debated. Mitrovica [1996] noted the Haskell constraint applies effectively to mantle depths of ~ 1000 – 1200 km, while Paulson and Richards [2009] drew attention to the trade-off between radial viscosity contrast and layer thickness: models favoring a coarse subdivision of the mantle into two layers separated at the 670 km phase transition will naturally obtain modest viscosity contrasts, while providing an equally good fit to the data as models with a thin layer and strong viscos-

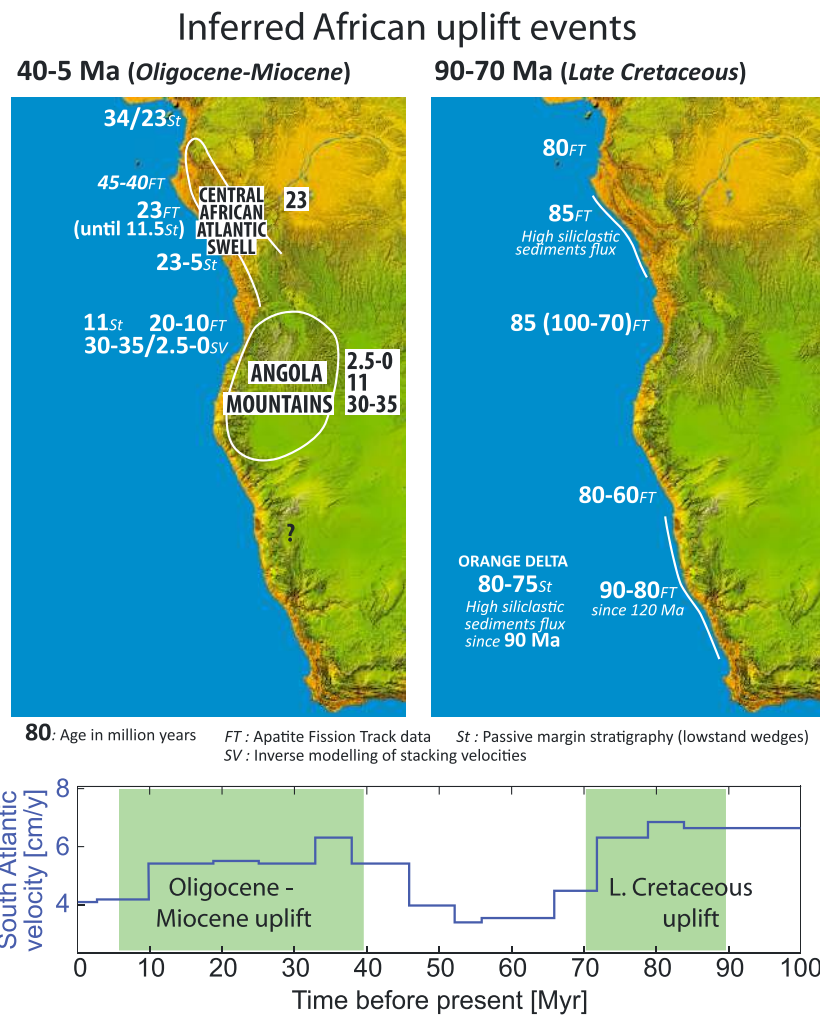


Figure 7. Main uplift events in Oligocene-Miocene (5–40 Myr) and Late Cretaceous (70–90 Myr) time along Africa’s South Atlantic margin as inferred from a variety of techniques: thermochronology (FT), sequence stratigraphy (St), and inverse modeling of stacking velocities from seismic lines (SV). The bottom panel shows that times of widespread uplift (shaded intervals) correlate with times of faster spreading.

Topography in the South Atlantic realm has changed over time. *Japsen et al.* [2012a] and *Cogne et al.* [2011] document Late Cretaceous and Eocene uplift events along the Brazilian coast. *MacGregor* [2012] summarizes margin uplifts for South America and Africa in Late Cretaceous and Oligocene. Since the seminal work by *King* [1955] a consensus exists [e.g., *Partridge and Maud*, 1987] that Southern Africa’s topography had experienced successive phases of planation by scarp retreat that produced low-relief pediplain that could be correlated across the continent (e.g., the Gondwana and the African surface). *King* [1955] proposed that episodic regional uplift caused these events.

The African side of the South Atlantic has three main relief elements: South African Plateau, Angola Mountains, and Congo-Cameroon Atlantic Swell. The uplift ages of these structures have been debated with three main scenarios. (1) Inheritance from Atlantic rifting [e.g., *Gilchrist et al.*, 1994], (2) Late Cretaceous [e.g., *de Wit*, 2007], and (3) Oligo-Miocene [e.g., *Burke and Gunnell*, 2008]. Geologic data (Figure 7) now suggest two main uplift periods, Late Cretaceous and Oligo-Miocene, with different amplitudes from South Africa to Cameroon. Late Cretaceous uplifts are documented by apatite fission track (AFT) data in Gabon [*Walgenwitz et al.*, 1992], South Africa-Namibia [*Gallagher and Brown*, 1999a, 1999b; *Kounov et al.*, 2009; *Raab et al.*, 2002, 2005; *Stanley et al.*, 2013], and Equatorial Guinea [*Turner et al.*, 2008]. Significant vertical displacement is also confirmed by numerous lowstand wedges along the margins [*Hartwig et al.*, 2012; *Hirsch et al.*, 2010;

McMillan, 2003; Paton *et al.*, 2008]. Supporting evidence comes from siliciclastic flux measurements. While these record continental denudation, not necessarily uplift, they are consistent with a major Late Cretaceous denudation event [Anka *et al.*, 2010; Guillocheau *et al.*, 2012; Leturmy *et al.*, 2003; MacGregor, 2012; Seranne and Anka, 2005].

The Oligo-Miocene uplift is also documented on AFT data along the Congo-Cameroon Atlantic Swell [Walgenwitz *et al.*, 1992] and the Angola Mountains [Jackson *et al.*, 2005], confirming the pioneering work of Lunde *et al.* [1992]. On the Angola margin, inverse modeling of stacking velocities along offshore seismic lines [Al-Hajri *et al.*, 2009; Walford and White, 2005] finds two major uplifts in early Oligocene and Pleistocene. Lowstand wedges and incised canyons were preserved along the Congo Delta [Anka *et al.*, 2009], and the Cameroon-Gabon margins, with canyon incision around the Eo-Oligocene boundary in Cameroon and major lowstand wedges in early Miocene [Manga, 2008; Rasmussen, 1996]. Along the Congo margin, paleowater depth reconstructions [Lavier *et al.*, 2001] and modeling of vertical movements [Lucazeau *et al.*, 2003] show similar uplift timing. Sedimentary flux analysis confirms the second denudation period [MacGregor, 2012; Seranne and Anka, 2005], with a strong increase along the Congo-Ogooue (Gabon) deltaic system [Anka *et al.*, 2009; Lavier *et al.*, 2001; Leturmy *et al.*, 2003].

These two major uplift events correlate with pulses in regional basin reactivation [Janssen *et al.*, 1995] and magmatic activity [Jelsma *et al.*, 2009; O'Connor *et al.*, 2012].

6. Discussion

Our results suggest that topographic variations of the Andes alone cannot fully account for the South Atlantic spreading changes. The most recent South Atlantic spreading reduction correlates with late Miocene Andean uplift. However, the elevation of the Andes was small in Late Cretaceous and Early Paleocene, relative to the present day, and presumably did not vary much in time. Thus, the pronounced early Tertiary spreading rate variations in the South Atlantic are not easily linked to elevation changes in the Andes.

At the same time, substantial evidence suggests that the bimodal spreading history of the South Atlantic is matched by a bimodal history of uplift on the South American and African sides of the South Atlantic [MacGregor, 2012]. A linkage between changes in horizontal and vertical motion is expected if temporal variations in upper mantle flow arise from temporal variations of pressure gradients in the asthenosphere. In this case, the evolving flow field would be associated with evolving basal shear forces and nonisostatic vertical motion that is dynamic topography.

6.1. Unmodeled Effects

We must emphasize that our force balance models and our fluid dynamic analysis of upper mantle flow are highly simplified. We have assumed a rigid plate overlying an incompressible Newtonian asthenosphere of constant thickness, disregarding among others the complex 3-D structure of the asthenosphere in the South Atlantic region that is imaged, for instance, by our tomographic study [Colli *et al.*, 2013]. Furthermore, we did not account for the complex rheological behavior of mantle material, and we considered the momentum equation alone, without coupling it to the heat and mass conservation equations in a self-consistent and time-dependent model. At this stage, however, we believe it is prudent to explore simple models of the South Atlantic region, aimed at providing physical insight, before moving to complex computational simulations that carry their own limitations. For example, a fully time-dependent geodynamic model of the plate tectonic evolution of the South Atlantic region would require the choice of an appropriate initial condition. While fluid dynamic inverse theory of mantle convection has been developed during the last decade [Bunge *et al.*, 2003; Ismail-Zadeh *et al.*, 2004], its application to the initial condition problem with real geophysical data remains challenging.

In our analysis of South Atlantic spreading variations, we did not account for changes in plate geometry offshore of the western margin of South America, which acquired its current shape since the Neogene as evidenced by paleomagnetic and geodetic studies [e.g., Allmendinger *et al.*, 2005, and references therein]. Paleoplate configurations recently published by Müller *et al.* [2008] and Seton *et al.* [2012], see Figure 8, suggest that plate motion was oblique along the central and northern Chilean margin before the Eocene, when the current subduction geometry was established. While it is not obvious how this plate geometry change would induce a deceleration and subsequent acceleration in South Atlantic spreading rates around the

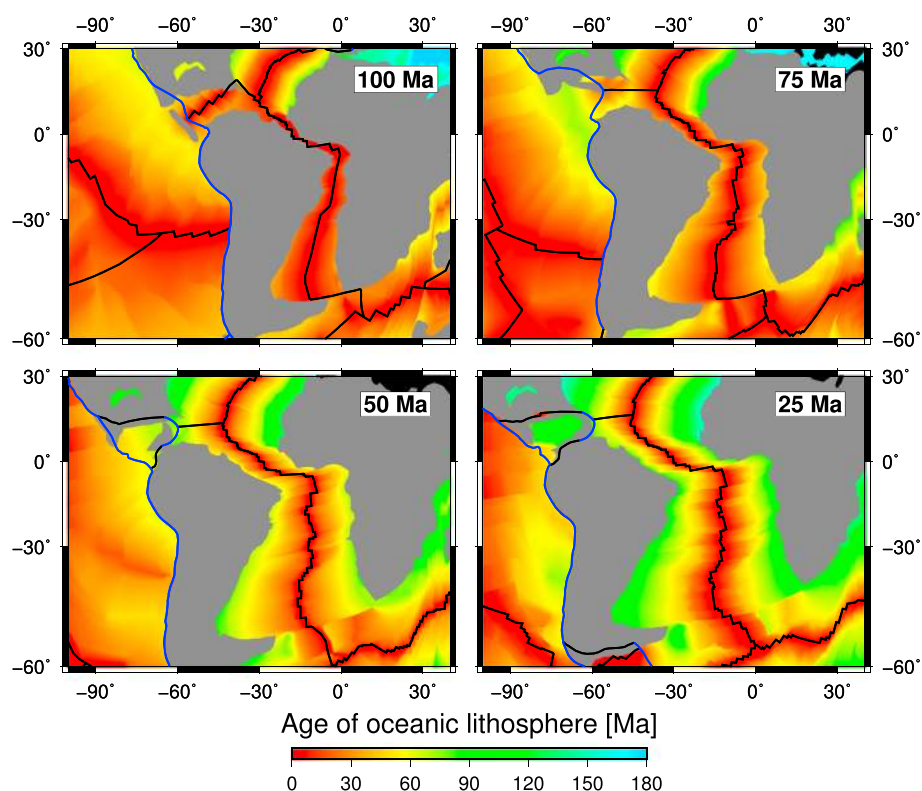


Figure 8. Plate configurations and ocean floor age in the South Atlantic region for four time periods (100 to 25 Myr) from Müller *et al.* [2008]. Note that oblique subduction off western South America is inferred to have changed into the current trench-perpendicular subduction from the Eocene (≈ 50 Myr) on, with a corresponding change from trench-parallel to trench-perpendicular motion.

Cretaceous/Tertiary boundary, or how this would explain the recent Eo-Oligocene uplift events recorded on the African continent, its influence should be investigated further.

We also assumed a constant friction coefficient of the South American plate boundaries, including the Andean margin, for the Cenozoic. The friction coefficient of megathrusts and marine plate margins could be regulated by the amount of sediments delivered to the margin—with the highest coefficient associated with sediment-starved margins, such as the present-day Chilean trench offshore the Altiplano-Puna Plateaus [Lamb, 2006; Seno, 2009]. Although semiarid climatic conditions prevailed during most of the Paleocene along the northernmost Chilean fore arc, Hartley [2003] proposed increased local aridity since the Oligocene as a dominant control on the rise of the Andean Plateau. This calls for a reduction of the amount of sediments transported from the fore arc into the trench and a subsequent increase of the interplate friction coefficient [Lamb and Davis, 2003; Oncken *et al.*, 2006]. However, variations of the effective friction coefficient along plate margins are unlikely to exceed 0.06 [Iaffaldano, 2012]. Moreover, any such variations along the Andean margin would have been restricted to a relatively minor portion of the total South American plate boundary. It is thus reasonable to expect no significant impact upon the torque balance and kinematics of the South American plate [e.g., Iaffaldano and Bunge, 2008].

6.2. Implications

Our results suggest it is possible to exploit the oceanic spreading record to quantify some of the forces involved in driving and resisting plate motion. Plate tectonics explains the piecewise constant nature of surface velocities on our planet [DeMets *et al.*, 1994], but the nature and magnitude of the driving and resisting forces remain obscure. The difficulty stems from three sources. First, the mantle buoyancy forces are not well known, although combining mantle convection simulations with mantle mineralogy models [Piazzoni *et al.*, 2007] may shed light on how to interpret mantle seismic structure in terms of density anomalies [Forte *et al.*, 2010; Schuberth *et al.*, 2009a, 2009b, 2012]. Second, we lack robust descriptions of the mantle

deformation behavior in the regime of low strain rates, high temperature, and high pressure that characterizes the deep Earth. Theoretical progress from multiscale material modeling [Castelnau *et al.*, 2010] may allow one to augment experimental work to better understand from first principle the deformation of mantle minerals [Ammann *et al.*, 2010; Cordier *et al.*, 2012]. The third challenge reflects the fact that the inertia of moving plates is negligible so that tectonic forces balance everywhere on Earth. Our ability to consider past and present plate velocities is thus essential to quantify the forces, because plate motion changes are necessarily driven by changes in the driving or resisting forces.

7. Conclusions

We have investigated the South Atlantic region in terms of spreading history, Andean topographic evolution, and upper mantle seismic structure, focusing on prominent short-term spreading velocity changes recorded in the basin. The far-field effects of the Andes on the South Atlantic spreading record are relatively straightforward. Rapid Andean topographic growth in the Miocene correlates with a recent reduction in South Atlantic spreading velocity, likely due to increased plate boundary forcing associated with the newly elevated topography. The twofold reduction in South Atlantic spreading velocity and subsequent renewed vigorous spreading at the Cretaceous/Tertiary boundary, in contrast, lack such correlation, as Andean paleoelevation at the time presumably was low. Torque balance models demonstrate that the Late Cretaceous/Tertiary spreading changes could arise from variations in basal drag associated with unsteady asthenosphere flow. The magnitude of the pressure-induced mantle flow velocities compares well with those required from independent considerations to maintain South American plate motion through basal shear. Predictions from our models for temporal changes in regional topography, due to temporal changes in pressure gradients and upper mantle flow, appear to agree with geologic and geophysical observations, including episodes of passive margin uplift, regional basin reactivation, and magmatic activity.

Acknowledgments

No new data were produced during this work. All data used come from the sources referenced in the text. We would like to thank Seth Stein, Adrian Lenardic, and an anonymous reviewer for their thoughtful and constructive reviews, and Peter Japsen for helpful discussions. The work of Lorenzo Colli, Hans-Peter Bunge, and Maria Chiara Bianchi was funded by the German Research Foundation (DFG) within the priority program SPP 1375—SAMPLE. Stuart Clark and Mark Smethurst conducted the work as part of a research grant from Statoil. Giampiero Iaffaldano acknowledges support from the Ringwood Fellowship at the Australian National University. François Guillocheau would like to thank the Agence Nationale de la Recherche (ANR-French Research National Agency) for funding the TopoAfrica project. The work of Lorenzo Colli was partially supported by COST Action ES0701.

References

- Al-Hajri, Y., N. White, and S. Fishwick (2009), Scales of transient convective support beneath Africa, *Geology*, 37(10), 883–886, doi:10.1130/G25703A.1.
- Allmendinger, R., R. Smalley, M. Bevis, H. Caprio, and B. Brooks (2005), Bending the Bolivian orocline in real time, *Geology*, 33(11), 905–908, doi:10.1130/G21779.1.
- Amante, C., and B. W. Eakins (2009), *ETOPO1 1 Arc-Minute Global Relief Model: Procedures, Data Sources and Analysis*, NOAA Technical Memorandum NESDIS NGDC-24, U.S. Dept. of Commerce, National Oceanic and Atmospheric Administration, National Environmental Satellite, Data, and Information Service, National Geophysical Data Center, Marine Geology and Geophysics Division, Boulder, Colo.
- Ammann, M. W., J. P. Brodholt, J. Wookey, and D. P. Dobson (2010), First-principles constraints on diffusion in lower-mantle minerals and a weak D" layer, *Nature*, 465(7297), 462–465, doi:10.1038/nature09052.
- Anderson, D. L. (1982), Hotspots, polar wander, Mesozoic convection and the geoid, *Nature*, 297, 391–393.
- Anderson, D. L., and C. Sammis (1970), Partial melting in the upper mantle, *Phys. Earth Planet. Inter.*, 3, 41–50, doi:10.1016/0031-9201(70)90042-7.
- Anka, Z., M. Seranne, M. Lopez, M. Scheck-Wenderoth, and B. Savoye (2009), The long-term evolution of the Congo deep-sea fan: A basin-wide view of the interaction between a giant submarine fan and a mature passive margin (ZaiAngo project), *Tectonophysics*, 470(1–2), 42–56, doi:10.1016/j.tecto.2008.04.009.
- Anka, Z., M. Seranne, and R. di Primio (2010), Evidence of a large upper-Cretaceous depocentre across the Continent-Ocean boundary of the Congo-Angola basin. Implications for palaeo-drainage and potential ultra-deep source rocks, *Mar. Pet. Geol.*, 27(3), 601–611, doi:10.1016/j.marpetgeo.2009.08.015.
- Barke, R., and S. Lamb (2006), Late Cenozoic uplift of the Eastern Cordillera, Bolivian Andes, *Earth Planet. Sci. Lett.*, 249(3–4), 350–367, doi:10.1016/j.epsl.2006.07.012.
- Barnes, J., T. Ehlers, N. McQuarrie, P. O'Sullivan, and J. Pelletier (2006), Eocene to recent variations in erosion across the central Andean fold-thrust belt, northern Bolivia: Implications for plateau evolution, *Earth Planet. Sci. Lett.*, 248(1–2), 118–133, doi:10.1016/j.epsl.2006.05.018.
- Barrell, J. (1914), The strength of the Earth's crust part VI Relations of isostatic movements to a sphere of weakness—The asthenosphere, *J. Geol.*, 22(7), 655–683.
- Becker, T. W., and L. Boschi (2002), A comparison of tomographic and geodynamic mantle models, *Geochem. Geophys. Geosyst.*, 3(1), 1003, doi:10.1029/2001GC000168.
- Bond, G. (1978), Evidence for late tertiary uplift of africa relative to North-America, South-America, Australia and Europe, *J. Geol.*, 86(1), 47–65.
- Braun, J. (2010), The many surface expressions of mantle dynamics, *Nat. Geosci.*, 3(12), 825–833, doi:10.1038/NGEO1020.
- Buck, W. R., C. Small, and W. B. F. Ryan (2009), Constraints on asthenospheric flow from the depths of oceanic spreading centers: The East Pacific Rise and the Australian-Antarctic discordance, *Geochem. Geophys. Geosyst.*, 10, Q09007, doi:10.1029/2009GC002373.
- Bullard, E., J. Everett, and A. Smith (1965), The fit of the continents around the Atlantic, *Philos. Trans. R. Soc. London, Ser. A*, 258(1088), 41–51, doi:10.1098/rsta.1965.0020.
- Bunge, H.-P. (2005), Low plume excess temperature and high core heat flux inferred from non-adiabatic geotherms in internally heated mantle circulation models, *Phys. Earth Planet. Inter.*, 153(1–3), 3–10, doi:10.1016/j.pepi.2005.03.017.
- Bunge, H.-P., M. A. Richards, and J. R. Baumgardner (1996), Effect of depth-dependent viscosity on the planform of mantle convection, *Nature*, 379, 436–438.

- Bunge, H.-P., M. A. Richards, C. Lithgow-Bertelloni, J. R. Baumgardner, S. P. Grand, and B. A. Romanowicz (1998), Time scales and heterogeneous structure in geodynamic Earth models, *Science*, 280(5360), 91–95, doi:10.1126/science.280.5360.91.
- Bunge, H.-P., Y. Ricard, and J. Matas (2001), Non-adiabaticity in mantle convection, *Geophys. Res. Lett.*, 28(5), 879–882.
- Bunge, H.-P., C. R. Hagelberg, and B. J. Travis (2003), Mantle circulation models with variational data assimilation: Inferring past mantle flow and structure from plate motion histories and seismic tomography, *Geophys. J. Int.*, 152(2), 280–301, doi:10.1046/j.1365-246X.2003.01823.x.
- Burke, K., and Y. Gunnell (2008), *The African Erosion Surface: A Continental-Scale Synthesis of Geomorphology, Tectonics, and Environmental Change Over the Past 180 Million Years*, Geol. Soc. Am., Boulder, Colo.
- Busse, F. H., M. A. Richards, and A. Lenardic (2006), A simple model of high Prandtl and high Rayleigh number convection bounded by thin low-viscosity layers, *Geophys. J. Int.*, 164, 160–167, doi:10.1111/j.1365-246X.2005.02836.x.
- Cande, S. C., J. L. LaBrecque, and W. F. Haxby (1988), Plate kinematics of the South Atlantic: Chron C34 to present, *J. Geophys. Res.*, 93(B11), 12,479–13,492.
- Carena, S., and C. Moder (2009), The strength of faults in the crust in the western United States, *Earth Planet. Sci. Lett.*, 287(3–4), 373–384, doi:10.1016/j.epsl.2009.08.021.
- Castelnau, O., P. Cordier, R. A. Lebensohn, S. Merkel, and P. Raterron (2010), Microstructures and rheology of the Earth's upper mantle inferred from a multiscale approach, *C.R. Phys.*, 11(3), 304–315, doi:10.1016/j.crhy.2010.07.011.
- Cathles, L. (1975), *The Viscosity of the Earth's Mantle*, Princeton Univ. Press, New Jersey.
- Channell, J. E. T., E. Erba, M. Nakanishi, and K. Tamaki (1995), Late Jurassic-Early Cretaceous time scales and oceanic magnetic anomaly block models, in *Geochronology, Time Scales and Global Stratigraphic Correlation*, vol. 54, edited by W. A. Bregggen et al., pp. 51–63, SEPM (Society for Sedimentary Geology) Spec. Publ., Tulsa, Okla.
- Charrier, R. (2007), Tectonostratigraphic evolution of the Andean orogen in Chile, in *The Geology of Chile*, edited by T. Moreno and W. Gibbons. *Geol. Soc. London Spec. Publ.*, 21–114.
- Chase, C. G. (1979), Asthenospheric counterflow—A kinematic model, *Geophys. J. R. Astron. Soc.*, 56(1), 1–18, doi:10.1111/j.1365-246X.1979.tb04764.x.
- Coffin, M. F., L. M. Gahagan, and L. A. Lawver (1998), Present-day plate boundary digital data compilation, *Tech. Rep. 174*, Univ. of Tex. Inst. for Geophysics, Austin.
- Cogne, N., K. Gallagher, and P. R. Cobbold (2011), Post-rift reactivation of the onshore margin of southeast Brazil: Evidence from apatite (U-Th)/He and fission-track data, *Earth Planet. Sci. Lett.*, 309(1–2), 118–130, doi:10.1016/j.epsl.2011.06.025.
- Colli, L., A. Fichtner, and H.-P. Bunge (2013), Full waveform tomography of the upper mantle in the South Atlantic region: Evidence for pressure-driven westward flow in a shallow asthenosphere, *Tectonophysics*, 604, 26–40.
- Cordier, P., J. Amodeo, and P. Carrez (2012), Modelling the rheology of MgO under Earth's mantle pressure, temperature and strain rates, *Nature*, 481(7380), 177–180, doi:10.1038/nature10687.
- Cornejo, P. (2003), The K-T compressive deformation event in northern Chile 24–27°S, in *10th Geological Congress*, Actas, CD-Rom, Sesión Temática 1, Concepcion Chile.
- Crosby, A. G., D. McKenzie, and J. G. Sclater (2006), The relationship between depth, age and gravity in the oceans, *Geophys. J. Int.*, 166(2), 553–573.
- Davies, D. R., S. Goes, J. H. Davies, B. S. A. Schuberth, H.-P. Bunge, and J. Ritsema (2012), Reconciling dynamic and seismic models of Earth's lower mantle: The dominant role of thermal heterogeneity, *Earth Planet. Sci. Lett.*, 353–354, 253–269, doi:10.1016/j.epsl.2012.08.016.
- Davies, G. (1999), *Dynamic Earth: Plates, Plumes and Mantle Convection*, Cambridge Univ. Press, New York.
- de Wit, M. (2007), The Kalahari epeirogeny and climate change: Differentiating cause and effect from core to space, *S. Afr. J. Geol.*, 110(2–3), 367–392, doi:10.2113/gssajg.110.2-3.367.
- Debayle, E., B. Kennett, and K. Priestley (2005), Global azimuthal seismic anisotropy and the unique plate-motion deformation of Australia, *Nature*, 433, 509–512, doi:10.1038/nature03247.
- DeMets, C., R. Gordon, D. Argus, and S. Stein (1994), Effect of recent revisions to the geomagnetic reversal time-scale on estimates of current plate motions, *Geophys. Res. Lett.*, 21(20), 2191–2194, doi:10.1029/94GL02118.
- Duncan, R. A., and M. A. Richards (1991), Hotspots, mantle plumes, flood basalts, and true polar wander, *Rev. Geophys.*, 29(1), 31–50, doi:10.1029/90RG02372.
- Dziewonski, A. M. (2005), The robust aspects of global seismic tomography, *Geol. Soc. Am. Spec. Pap.*, 388, 147–154, doi:10.1130/0-8137-2388-4.147.
- Ege, H., E. R. Sobel, E. Scheuber, and V. Jacobshagen (2007), Exhumation history of the southern Altiplano Plateau (southern Bolivia) constrained by apatite fission track thermochronology, *Tectonics*, 26(1), TC1004, doi:10.1029/2005TC001869.
- Forsyth, D., and S. Uyeda (1975), Relative importance of driving forces of plate motion, *Geophys. J. R. Astron. Soc.*, 43(1), 163–200, doi:10.1111/j.1365-246X.1975.tb00631.x.
- Forté, A. M., S. Quere, R. Moucha, N. A. Simmons, S. P. Grand, J. X. Mitrovica, and D. B. Rowley (2010), Joint seismic-geodynamic-mineral physical modelling of African geodynamics: A reconciliation of deep-mantle convection with surface geophysical constraints, *Earth Planet. Sci. Lett.*, 295(3–4), 329–341, doi:10.1016/j.epsl.2010.03.017.
- Fowler, C. (1990), *The Solid Earth: An Introduction to Global Geophysics*, Cambridge Univ. Press, Cambridge.
- French, S., V. Lekic, and B. Romanowicz (2013), Waveform tomography reveals channeled flow at the base of the oceanic asthenosphere, *Science*, 342, 227–330, doi:10.1126/science.1241514.
- Gallagher, K., and R. Brown (1999a), Denudation and uplift at passive margins: The record on the Atlantic Margin of Southern Africa, *Philos. T. Roy. Soc. A*, 357(1753), 835–857.
- Gallagher, K., and R. Brown (1999b), The Mesozoic denudation history of the Atlantic margins of Southern Africa and southeast Brazil and the relationship to offshore sedimentation, in *The Oil and Gas Habitats of the South Atlantic*, edited by N. R. Cameron, and R. H. Bate, and V. S. Clure. *Geol. Soc. London Spec. Publ.*, 153, 41–53.
- Gansser, A. (1973), Facts and theories on the Andes, *J. Geol. Soc. London*, 129, 93–131.
- Garzone, C. N., P. Molnar, J. C. Libarkin, and B. J. MacFadden (2006), Rapid late Miocene rise of the Bolivian Altiplano: Evidence for removal of mantle lithosphere, *Earth Planet. Sci. Lett.*, 241(3–4), 543–556, doi:10.1016/j.epsl.2005.11.026.
- Ghosh, P., C. N. Garzone, and J. M. Eiler (2006), Rapid uplift of the Altiplano revealed through C-13-O-18 bonds in paleosol carbonates, *Science*, 311(5760), 511–515, doi:10.1126/science.1119365.
- Gilchrist, A., H. Kooi, and C. Beaumont (1994), Post-Gondwana geomorphic evolution of southwestern Africa—Implications for the controls on landscape development from observations and numerical experiments, *J. Geophys. Res.*, 99(B6), 12,211–12,228, doi:10.1029/94JB00046.

- Gillis, R. J., B. K. Horton, and M. Grove (2006), Thermochronology, geochronology, and upper crustal structure of the Cordillera Real: Implications for Cenozoic exhumation of the central Andean Plateau, *Tectonics*, 25(6), TC6007, doi:10.1029/2005TC001887.
- Gradstein, F. M., J. G. Ogg, A. G. Smith, W. Bleeker, and L. J. Lourens (2004), A new geologic time scale, with special reference to Precambrian and Neogene, *Episodes*, 27(2), 83–100.
- Grand, S. P. (2002), Mantle shear-wave tomography and the fate of subducted slabs, *Philos. Trans. R. Soc. London, Ser. A*, 360(1800), 2475–2491.
- Gregory-Wodzicki, K. (2000), Uplift history of the Central and Northern Andes: A review, *Geol. Soc. Am. Bull.*, 112(7), 1091–1105, doi:10.1130/0016-7606(2000)112<1091:UHOTCA>2.3.CO;2.
- Guillocheau, F., D. Rouby, C. Robin, C. Helm, N. Rolland, C. L. C. de Veslud, and J. Braun (2012), Quantification and causes of the terrigenous sediment budget at the scale of a continental margin: A new method applied to the Namibia-South Africa margin, *Basin Res.*, 24(1), 3–30, doi:10.1111/j.1365-2117.2011.00511.x.
- Harig, C., S. Zhong, and F. J. Simons (2010), Constraints on upper mantle viscosity from the flow-induced pressure gradient across the Australian continental keel, *Geochem. Geophys. Geosyst.*, 11, Q06004, doi:10.1029/2010GC003038.
- Hartley, A. (2003), Andean uplift and climate change, *J. Geol. Soc. London*, 160(1), 7–10, doi:10.1144/0016-764902-083.
- Hartwig, A., Z. Anka, and R. di Primio (2012), Evidence of a widespread paleo-pockmarked field in the Orange Basin: An indication of an early Eocene massive fluid escape event offshore South Africa, *Mar. Geol.*, 332, 222–234, doi:10.1016/j.margeo.2012.07.012.
- Haskell, N. A. (1935), The motion of a viscous fluid under a surface load, *J. Appl. Phys.*, 6(1), 265–269, doi:10.1063/1.1745329.
- Hirsch, K. K., M. Scheck-Wenderoth, J.-D. van Wees, G. Kuhlmann, and D. A. Paton (2010), Tectonic subsidence history and thermal evolution of the Orange Basin, *Mar. Pet. Geol.*, 27(3), 565–584, doi:10.1016/j.marpetgeo.2009.06.009.
- Höink, T., and A. Lenardic (2008), Three-dimensional mantle convection simulations with a low-viscosity asthenosphere and the relationship between heat flow and the horizontal length scale of convection, *Geophys. Res. Lett.*, 35, L10304, doi:10.1029/2008GL033854.
- Höink, T., and A. Lenardic (2010), Long wavelength convection, Poiseuille-Couette flow in the low-viscosity asthenosphere and the strength of plate margins, *Geophys. J. Int.*, 180(1), 23–33, doi:10.1111/j.1365-246X.2009.04404.x.
- Höink, T., A. M. Jellinek, and A. Lenardic (2011), Viscous coupling at the lithosphere-asthenosphere boundary, *Geochem. Geophys. Geosyst.*, 12, Q0AK02, doi:10.1029/2011GC003698.
- Hoorn, C., et al. (2010), Amazonia through time: Andean uplift, climate change, landscape evolution, and biodiversity, *Science*, 330(6006), 927–931, doi:10.1126/science.1194585.
- Houser, C., G. Masters, P. Shearer, and G. Laske (2008), Shear and compressional velocity models of the mantle from cluster analysis of long-period waveforms, *Geophys. J. Int.*, 174(1), 195–212, doi:10.1111/j.1365-246X.2008.03763.x.
- Husson, L., and Y. Ricard (2004), Stress balance above subduction: Application to the Andes, *Earth Planet. Sci. Lett.*, 222(3–4), 1037–1050, doi:10.1016/j.epsl.2004.03.041.
- Husson, L., C. P. Conrad, and C. Faccenna (2012), Plate motions, Andean orogeny, and volcanism above the South Atlantic convection cell, *Earth Planet. Sci. Lett.*, 317, 126–135, doi:10.1016/j.epsl.2011.11.040.
- Iaffaldano, G. (2012), The strength of large-scale plate boundaries: Constraints from the dynamics of the Philippine Sea plate since ~5Ma, *Earth Planet. Sci. Lett.*, 357–358, 21–30, doi:10.1016/j.epsl.2012.09.018.
- Iaffaldano, G., and H.-P. Bunge (2008), Strong plate coupling along the Nazca-South America convergent margin, *Geology*, 36(6), 443–446, doi:10.1130/G24489A.1.
- Iaffaldano, G., and H.-P. Bunge (2009), Relating rapid plate-motion variations to plate-boundary forces in global coupled models of the mantle/lithosphere system: Effects of topography and friction, *Tectonophysics*, 474(1–2), 393–404, doi:10.1016/j.tecto.2008.10.035.
- Iaffaldano, G., H.-P. Bunge, and T. H. Dixon (2006), Feedback between mountain belt growth and plate convergence, *Geology*, 34(10), 893–896, doi:10.1130/G22661.1.
- Iaffaldano, G., T. Bodin, and M. Sambridge (2012), Reconstructing plate-motion changes in the presence of finite-rotations noise, *Nat. Commun.*, 3, 1048, doi:10.1038/ncomms2051.
- Ismail-Zadeh, A., G. Schubert, I. Tsepelev, and A. Korotkii (2004), Inverse problem of thermal convection: Numerical approach and application to mantle plume restoration, *Phys. Earth Planet. Inter.*, 145(1–4), 99–114, doi:10.1016/j.pepi.2004.03.006.
- Jackson, M., M. Hudec, and K. Hegarty (2005), The great West African Tertiary coastal uplift: Fact or fiction? A perspective from the Angolan divergent margin, *Tectonics*, 24(6), TC6014, doi:10.1029/2005TC001836.
- Jaillard, E. (1994), Kimmeridgian to Paleocene tectonic and geodynamic evolution of the Peruvian (and Ecuadorian) margin, in *Cretaceous Tectonics of the Andes*, edited by J. A. Salfity, pp. 101–167, Earth Evol. Sci., Vieweg, Braunschweig, Germany.
- Jaillard, E., and P. Soler (1996), Cretaceous to early Paleogene tectonic evolution of the northern Central Andes (0–18 degrees S) and its relations to geodynamics, *Tectonophysics*, 259(1–3), 41–53, doi:10.1016/0040-1951(95)00107-7.
- Janssen, M. E., R. A. Stephenson, and S. Cloetingh (1995), Temporal and spatial correlations between changes in plate motions and the evolution of rifted basins in Africa, *Geol. Soc. Am. Bull.*, 107(11), 1317–1332.
- Japsen, P., J. A. Chalmers, P. F. Green, and J. M. Bonow (2012a), Elevated, passive continental margins: Not rift shoulders, but expressions of episodic, post-rift burial and exhumation, *Global Planet. Change*, 90–91, 73–86, doi:10.1016/j.gloplacha.2011.05.004.
- Japsen, P., J. M. Bonow, P. F. Green, P. R. Cobbold, D. Chiossi, R. Lilletveit, L. P. Magnavita, and A. Pedreira (2012b), Episodic burial and exhumation in NE Brazil after opening of the South Atlantic, *Geol. Soc. Am. Bull.*, 124(5–6), 800–816, doi:10.1130/B30515.1.
- Jelsma, H., W. Barnett, S. Richards, and G. Lister (2009), Tectonic setting of kimberlites, *Lithos*, 112, 155–165, doi:10.1016/j.lithos.2009.06.030.
- Jones, A. G. (1982), Observations of the electrical asthenosphere beneath Scandinavia, *Tectonophysics*, 90(1–2), 37–55, doi:10.1016/0040-1951(82)90252-9.
- Karato, S., and H. Jung (1998), Water, partial melting and the origin of the seismic low velocity and high attenuation zone in the upper mantle, *Earth Planet. Sci. Lett.*, 157(3–4), 193–207, doi:10.1016/S0012-821X(98)00034-X.
- Karato, S.-I., and P. Wu (1993), Rheology of the upper mantle: A synthesis, *Science*, 260, 771–778.
- King, L. C. (1955), Pediplanation and isostasy: An example from South Africa, *Q. J. Geol. Soc. London*, 111, 353–359.
- Kounov, A., G. Viola, M. de Wit, and M. Andreoli (2009), Denudation along the Atlantic passive margin: New insights from apatite fission-track analysis on the western coast of South Africa, in *Thermochronological Methods: From Palaeotemperature Constraints to Landscape Evolution Models*, edited by F. Lisker, and B. Ventura, and U. A. Glasmacher, *Geol. Soc. London Spec. Publ.*, 324, 1–20.
- Kustowski, B., G. Ekstrom, and A. M. Dziewonski (2008), Anisotropic shear-wave velocity structure of the Earth's mantle: A global model, *J. Geophys. Res.*, 113, B06306, doi:10.1029/2007JB005169.
- Labails, C., T. H. Torsvik, C. Gaina, and R. M. Cocks (2009), Global plate polygons 2009. SPlates Model (version 2.0), *Tech. Rep. 2009.047*, NGU, Postboks 6315 Sluppen, 7491 Trondheim. [Available at <http://www.ngu.no/en-gb/>]

- Labrosse, S. (2002), Hotspots, mantle plumes and core heat loss, *Earth Planet. Sci. Lett.*, *199*(1–2), 147–156, doi:10.1016/S0012-821X(02)00537-X.
- Lamb, S. (2006), Shear stresses on megathrusts: Implications for mountain building behind subduction zones, *J. Geophys. Res.*, *111*(B7), B07401, doi:10.1029/2005JB003916.
- Lamb, S., and P. Davis (2003), Cenozoic climate change as a possible cause for the rise of the Andes, *Nature*, *425*(6960), 792–797, doi:10.1038/nature02049.
- Lavier, L., M. Steckler, and F. Brigaud (2001), Climatic and tectonic control on the Cenozoic evolution of the West African margin, *Mar. Geol.*, *178*(1–4), 63–80, doi:10.1016/S0025-3227(01)00175-X.
- Lekić, V., and B. Romanowicz (2011), Inferring upper-mantle structure by full waveform tomography with the spectral element method, *Geophys. J. Int.*, *185*, 799–831, doi:10.1111/j.1365-246X.2011.04969.x.
- Leturmy, P., F. Lucazeau, and F. Brigaud (2003), Dynamic interactions between the Gulf of Guinea passive margin and the Congo River drainage basin: 1. Morphology and mass balance, *J. Geophys. Res.*, *108*(B8), 2383, doi:10.1029/2002JB001927.
- Lithgow-Bertelloni, C., and M. A. Richards (1995), Cenozoic plate driving forces, *Geophys. Res. Lett.*, *22*(11), 1317–1320, doi:10.1029/95GL01325.
- Lucazeau, F., F. Brigaud, and P. Leturmy (2003), Dynamic interactions between the Gulf of Guinea passive margin and the Congo River drainage basin: 2. Isostasy and uplift, *J. Geophys. Res.*, *108*(B8), 2384, doi:10.1029/2002JB001928.
- Lunde, G., K. Aubert, O. Lauritzen, and E. Lorange (1992), Tertiary uplift of the Kwanza Basin in Angola, in *Géologie Africaine: Coll. Géol. Libreville, Recueil des Communications, 6–8 May 1991*, edited by R. Curnelle, pp. 99–117, Elf-Aquitaine, Boussens, France.
- MacGregor, D. S. (2012), Late Cretaceous-Cenozoic sediment and turbidite reservoir supply to South Atlantic margins, in *Conjugate Divergent Margins*, edited by W. U. Mohriak et al., *Geol. Soc. London Spec. Publ.*, *369*, 20.
- Manga, C. S. (2008), Stratigraphy, structure and prospectivity of the Southern onshore Douala Basin, Cameroon, Central Africa, in *Cameroon and Neighboring Basins in the Gulf of Guinea (Petroleum Geology Tectonics Geophysics Paleontology and Hydrogeology)*, *Africa Geosci. Rev. Spec. Publ.*, edited by M. J. Ntamak-Nida, G. E. Ekodeck, and M. Guiraud, pp. 13–37, Malakoff, France.
- McMillan, I. (2003), Foraminiferally defined biostratigraphic episodes and sedimentation pattern of the Cretaceous drift succession (Early Barremian to Late Maastrichtian) in seven basins on the South African and southern Namibian continental margin, *S. Afr. J. Sci.*, *99*(11–12), 537–576.
- Mitrovica, J. X. (1996), Haskell [1935] revisited, *J. Geophys. Res.*, *101*(B1), 555–569, doi:10.1029/95JB03208.
- Mittelstaedt, E., and P. J. Tackley (2006), Plume heat flow is much lower than CMB heat flow, *Earth Planet. Sci. Lett.*, *241*(1–2), 202–210, doi:10.1016/j.epsl.2005.10.012.
- Molnar, P., and J. M. Stock (2009), Slowing of India's convergence with Eurasia since 20 Ma and its implications for Tibetan mantle dynamics, *Tectonics*, *28*, TC3001, doi:10.1029/2008TC002271.
- Moulin, M., D. Aslanian, and P. Unternehr (2010), A new starting point for the South and Equatorial Atlantic Ocean, *Earth Sci. Rev.*, *98*(1–2), 1–37.
- Mpodozis, C., C. Arriagada, M. Basso, P. Roperch, P. Cobbold, and M. Reich (2005), Late Mesozoic to paleogene stratigraphy of the Salar de Atacama Basin, Antofagasta, Northern Chile: Implications for the tectonic evolution of the Central Andes, *Tectonophysics*, *399*(1–4), 125–154, doi:10.1016/j.tecto.2004.12.019.
- Müller, R. D., J.-Y. Royer, and L. A. Lawver (1993), Revised plate motions relative to the hotspots from combined Atlantic and Indian Ocean hotspot tracks, *Geology*, *21*(3), 275, doi:10.1130/0091-7613(1993)021<0275:RPMRTT>2.3.CO;2.
- Müller, R. D., W. R. Roest, J. Y. Royer, L. M. Gahagan, and J. G. Sclater (1997), Digital isochrons of the world's ocean floor, *J. Geophys. Res.*, *102*, 3211–3214.
- Müller, R. D., J.-Y. Royer, S. C. Cande, W. R. Roest, and S. Maschenkov (1999), New constraints on the late Cretaceous/Tertiary plate tectonic evolution of the Caribbean, in *Caribbean Basins, Sedimentary Basins of the World*, vol. 4, edited by P. Mann, pp. 33–59, Elsevier, Amsterdam, doi:10.1016/S1874-5997(99)80036-7.
- Müller, R. D., M. Sdrolias, C. Gaina, and W. R. Roest (2008), Age, spreading rates, and spreading asymmetry of the world's ocean crust, *Geochem. Geophys. Geosyst.*, *9*(4), Q04006, doi:10.1029/2007GC001743.
- Nerlich, R., S. R. Clark, and H.-P. Bunge (2013), The Scotia Sea gateway: No outlet for Pacific mantle, *Tectonophysics*, *604*, 41–50, doi:10.1016/j.tecto.2012.08.023.
- Norabuena, E. O., T. H. Dixon, S. Stein, and C. G. A. Harrison (1999), Decelerating Nazca-South America and Nazca-Pacific Plate motions, *Geophys. Res. Lett.*, *26*(22), 3405–3408, doi:10.1029/1999GL005394.
- Nürnberg, D., and R. D. Müller (1991), The tectonic evolution of the South Atlantic from Late Jurassic to present, *Tectonophysics*, *191*(1), 21–53.
- Nyblade, A. A., and S. W. Robinson (1994), The African superswell, *Geophys. Res. Lett.*, *21*(9), 765–768.
- O'Connor, J. M., W. Jokat, A. P. le Roex, C. Class, J. R. Wijbrans, S. Kessling, K. F. Kuiper, and O. Nebel (2012), Hotspot trails in the South Atlantic controlled by plume and plate tectonic processes, *Nat. Geosci.*, *5*(10), 735–738, doi:10.1038/NGEO1583.
- Oncken, O., G. Chong, G. Franz, P. Giese, H.-J. Götze, V. A. Ramos, M. R. Strecker, and P. Wigger (2006), *The Andes: Active Subduction Orogeny*, *Frontiers in Earth Sciences*, Springer, Berlin Heidelberg, New York.
- O'Neill, C., D. Müller, and B. Steinberger (2005), On the uncertainties in hot spot reconstructions and the significance of moving hot spot reference frames, *Geochem. Geophys. Geosyst.*, *6*(4), Q04003, doi:10.1029/2004GC000784.
- Orts, S., and V. A. Ramos (2006), *Evidence of Middle to Late Cretaceous Compressive Deformation in the High Andes of Mendoza, Argentina*, 65, Backbone of the Americas, Abstracts With Programs, Patagonia to Alaska, GSA Special Meetings-AGA Publicaciones Especiales No. 5, Mendoza.
- Panning, M., and B. Romanowicz (2006), A three-dimensional radially anisotropic model of shear velocity in the whole mantle, *Geophys. J. Int.*, *167*(1), 361–379, doi:10.1111/j.1365-246X.2006.03100.x.
- Partridge, T. C., and R. R. Maud (1987), Geomorphic evolution of Southern Africa since the Mesozoic, *S. Afr. J. Geol.*, *90*(2), 179–208.
- Paton, D. A., D. van der Spuy, R. di Primio, and B. Horsfield (2008), Tectonically induced adjustment of passive-margin accommodation space: influence on the hydrocarbon potential of the Orange Basin, South Africa, *AAPG Bull.*, *92*(5), 589–609, doi:10.1306/12280707023.
- Paulson, A., and M. A. Richards (2009), On the resolution of radial viscosity structure in modelling long-wavelength postglacial rebound data, *Geophys. J. Int.*, *179*(3), 1516–1526, doi:10.1111/j.1365-246X.2009.04362.x.
- Phipps Morgan, J., and W. H. F. Smith (1992), Flattening of the sea-floor depth age curve as a response to asthenospheric flow, *Nature*, *359*(6395), 524–527, doi:10.1038/359524a0.
- Phipps Morgan, J., W. J. Morgan, Y.-S. Zhang, and W. H. F. Smith (1995), Observational hints for a plume-fed, suboceanic asthenosphere and its role in mantle convection, *J. Geophys. Res.*, *100*(B7), 12,753–12,767.

- Piazzoni, A. S., G. Steinle-Neumann, H. P. Bunge, and D. Dolejs (2007), A mineralogical model for density and elasticity of the Earth's mantle, *Geochem. Geophys. Geosyst.*, 8, Q11010, doi:10.1029/2007GC001697.
- Raab, M., R. Brown, K. Gallagher, A. Carter, and K. Weber (2002), Late Cretaceous reactivation of major crustal shear zones in northern Namibia: Constraints from apatite fission track analysis, *Tectonophysics*, 349(1–4), 75–92, doi:10.1016/S0040-1951(02)00047-1.
- Raab, M., R. Brown, K. Gallagher, K. Weber, and A. Gleadow (2005), Denudational and thermal history of the Early Cretaceous Brandberg and Okenyanya igneous complexes on Namibia's Atlantic passive margin, *Tectonics*, 24(3), TC3006, doi:10.1029/2004TC001688.
- Rasmussen, E. (1996), Structural evolution and sequence formation offshore South Gabon during the Tertiary, *Tectonophysics*, 266(1–4), 509–523, doi:10.1016/S0040-1951(96)00236-3.
- Richards, M. A., and B. H. Hager (1984), Geoid anomalies in a dynamic Earth, *J. Geophys. Res.*, 89(B7), 5987–6002, doi:10.1029/JB089iB07p05987.
- Rickers, F., A. Fichtner, and J. Trampert (2013), The Iceland-Jan Mayen plume system and its impact on mantle dynamics in the North Atlantic region: Evidence from full-waveform inversion, *Earth Planet. Sci. Lett.*, 367, 39–51, doi:10.1016/j.epsl.2013.02.022.
- Ritsema, J., A. Deuss, H. J. van Heijst, and J. H. Woodhouse (2011), S40RTS: A degree-40 shear-velocity model for the mantle from new Rayleigh wave dispersion, teleseismic traveltimes and normal-mode splitting function measurements, *Geophys. J. Int.*, 3(184), 1223–1236.
- Romanowicz, B., and Y. C. Gung (2002), Superplumes from the core-mantle boundary to the lithosphere: Implications for heat flux, *Science*, 296(5567), 513–516, doi:10.1126/science.1069404.
- Rousse, S., S. Gilder, D. Farber, B. McNulty, P. Patriat, V. Torres, and T. Sempere (2003), Paleomagnetic tracking of mountain building in the Peruvian Andes since 10 Ma, *Tectonics*, 22(5), 1048, doi:10.1029/2003TC001508.
- Schaber, K., H.-P. Bunge, B. S. A. Schubert, R. Malservisi, and A. Horbach (2009), Stability of the rotation axis in high-resolution mantle circulation models: Weak polar wander despite strong core heating, *Geochem. Geophys. Geosyst.*, 10, Q11W04, doi:10.1029/2009GC002541.
- Schildgen, T. F., K. V. Hodges, K. X. Whipple, P. W. Reiners, and M. S. Pringle (2007), Uplift of the western margin of the Andean Plateau revealed from canyon incision history, southern Peru, *Geology*, 35(6), 523–526, doi:10.1130/G23532A.1.
- Schubert, B. S. A., H.-P. Bunge, and J. Ritsema (2009a), Tomographic filtering of high-resolution mantle circulation models: Can seismic heterogeneity be explained by temperature alone?, *Geochem. Geophys. Geosyst.*, 10(5), Q05W03, doi:10.1029/2009GC002401.
- Schubert, B. S. A., H.-P. Bunge, G. Steinle-Neumann, C. Moder, and J. Oeser (2009b), Thermal versus elastic heterogeneity in high-resolution mantle circulation models with pyrolite composition: High plume excess temperatures in the lowermost mantle, *Geochem. Geophys. Geosyst.*, 10(1), Q01W01, doi:10.1029/2008GC002235.
- Schubert, B. S. A., C. Zanolli, and G. Nolet (2012), Synthetic seismograms for a synthetic Earth: Long-period P- and S-wave traveltime variations can be explained by temperature alone, *Geophys. J. Int.*, 188(3), 1393–1412, doi:10.1111/j.1365-246X.2011.05333.x.
- Sebrier, M., A. Lavenue, M. Fornari, and J.-P. Soulas (1988), Tectonics and uplift in the Central Andes (Peru, Bolivia and Northern Chile) from Eocene to Present, *Géodynamique*, 3, 85–106.
- Sempere, T., G. Herail, J. Oller, and M. Bonhomme (1990), Late Oligocene-early Miocene major tectonic crisis and related basins in Bolivia, *Geology*, 18(10), 946–949, doi:10.1130/0091-7613(1990)018<0946:LOEMMT>2.3.CO;2.
- Sempere, T., L. Marshall, S. Rivano, and E. Godoy (1994), Late Oligocene-early Miocene compressional tectosedimentary episode and associated land-mammal faunas in the Andes of central Chile and Adjacent Argentina (32–37°S), *Tectonophysics*, 229(3–4), 251–264, doi:10.1016/0040-1951(94)90032-9.
- Sempere, T., R. Butler, D. Richards, L. Marshall, W. Sharp, and C. Swisher (1997), Stratigraphy and chronology of Upper Cretaceous lower Paleogene strata in Bolivia and northwest Argentina, *Geol. Soc. Am. Bull.*, 109(6), 709–727, doi:10.1130/0016-7606(1997)109<0709:SACOU>2.3.CO;2.
- Sempere, T., A. Folguera, and M. Gerbault (2008), New insights into Andean evolution: An introduction to contributions from the 6th ISAG symposium (Barcelona, 2005), *Tectonophysics*, 459(1–4), 1–13, doi:10.1016/j.tecto.2008.03.011.
- Seno, T. (2009), Determination of the pore fluid pressure ratio at seismogenic megathrusts in subduction zones: Implications for strength of asperities and Andean-type mountain building, *J. Geophys. Res.*, 114, B05405, doi:10.1029/2008JB005889.
- Seranne, M., and Z. Anka (2005), South Atlantic continental margins of Africa: A comparison of the tectonic vs climate interplay on the evolution of equatorial West Africa and SW Africa margins, *J. Afr. Earth. Sci.*, 43(1–3), 283–300, doi:10.1016/j.jafrearsci.2005.07.010.
- Seton, M., et al. (2012), Global continental and ocean basin reconstructions since 200 Ma, *Earth Sci. Rev.*, 113(3–4), 212–270, doi:10.1016/j.earscirev.2012.03.002.
- Shapiro, N. M., and M. H. Ritzwoller (2002), Monte-Carlo inversion for a global shear-velocity model of the crust and upper mantle, *Geophys. J. Int.*, 151(1), 88–105, doi:10.1046/j.1365-246X.2002.01742.x.
- Shaw, P. R., and S. C. Cande (1990), High-resolution inversion for South Atlantic plate kinematics using joint altimeter and magnetic anomaly data, *J. Geophys. Res.*, 95(B3), 2625–2644.
- Silver, P., R. Russo, and C. Lithgow-Bertelloni (1998), Coupling of South American and African plate motion and plate deformation, *Science*, 279(5347), 60–63, doi:10.1126/science.279.5347.60.
- Simmons, N. A., A. M. Forte, and S. P. Grand (2006), Constraining mantle flow with seismic and geodynamic data: A joint approach, *Earth Planet. Sci. Lett.*, 246(1–2), 109–124, doi:10.1016/j.epsl.2006.04.003.
- Simmons, N. A., A. M. Forte, and S. P. Grand (2007), Thermochemical structure and dynamics of the African superplume, *Geophys. Res. Lett.*, 34(L02301), doi:10.1029/2006GL028009.
- Spetzler, J., J. Trampert, and R. Snieder (2002), The effect of scattering in surface wave tomography, *Geophys. J. Int.*, 149(3), 755–767, doi:10.1046/j.1365-246X.2002.01683.x.
- Stanley, J. R., R. M. Flowers, and D. R. Bell (2013), Kimberlite (U-Th)/he dating links surface erosion with lithospheric heating, thinning, and metasomatism in the southern African plateau, *Geology*, 41(12), 1243–1246, doi:10.1130/g34797.1.
- Steinberger, B., and T. H. Torsvik (2008), Absolute plate motions and true polar wander in the absence of hotspot tracks, *Nature*, 452(7187), 620–623, doi:10.1038/nature06824.
- Steinmann, G., C. I. Lissou, A. Sieberg, and R. Stappenbeck (1929), *Geologie von Peru*, Winters Universitätsbuchhandlung, Heidelberg.
- Suppe, J. (2007), Absolute fault and crustal strength from wedge tapers, *Geology*, 35(12), 1127–1130, doi:10.1130/G24053A.1.
- Tackley, P. J. (1996), On the ability of phase transitions and viscosity layering to induce long wavelength heterogeneity in the mantle, *Geophys. Res. Lett.*, 23(15), 1985–1988, doi:10.1029/96GL01980.
- Thouret, J.-C., G. Woerner, Y. Gunnell, B. Singer, X. Zhang, and T. Souriot (2007), Geochronologic and stratigraphic constraints on canyon incision and Miocene uplift of the Central Andes in Peru, *Earth Planet. Sci. Lett.*, 263(3–4), 151–166, doi:10.1016/j.epsl.2007.07.023.
- Torsvik, T. H., S. Rousse, C. Labails, and M. A. Smethurst (2009), A new scheme for the opening of the South Atlantic Ocean and the dissection of an Aptian salt basin, *Geophys. J. Int.*, 177(3), 1315–1333, doi:10.1111/j.1365-246X.2009.04137.x.

- Turner, J. P., P. F. Green, S. P. Holford, and S. R. Lawrence (2008), Thermal history of the Rio Muni (West Africa)-NE Brazil margins during continental breakup, *3-4*, 270, 354–367, doi:10.1016/j.epsl.2008.04.002.
- Walford, H., and N. White (2005), Constraining uplift and denudation of West African continental margin by inversion of stacking velocity data, *J. Geophys. Res.*, *110*, B04403, doi:10.1029/2003JB002893.
- Walgenwitz, F. R., J. P. Richert, and P. Charpentier (1992), Southwest African plate margin: Thermal history and geodynamical implications, in *Geologic Evolution of Atlantic Continental Rises*, edited by C. W. Poag and P. C. de Graciansky, pp. 20–45, Van Nostrand Reinhold, New York.
- Wang, Z., and F. A. Dahlen (1995), Validity of surface-wave ray theory on a laterally heterogeneous Earth, *Geophys. J. Int.*, *123*(3), 757–773, doi:10.1111/j.1365-246X.1995.tb06888.x.
- Weertman, J., and J. R. Weertman (1975), High-temperature creep of rock and mantle viscosity, *Annu. Rev. Earth Planet. Sci.*, *3*, 293–315, doi:10.1146/annurev.ea.03.050175.001453.
- Wiens, D. A., and S. Stein (1985), Implications of oceanic intraplate seismicity for plate stresses, driving forces and rheology, *Tectonophysics*, *116*(1–2), 143–162, doi:10.1016/0040-1951(85)90227-6.
- Winterbourne, J., A. Crosby, and N. White (2009), Depth, age and dynamic topography of oceanic lithosphere beneath heavily sedimented Atlantic margins, *Earth Planet. Sci. Lett.*, *287*(1–2), 137–151, doi:10.1016/j.epsl.2009.08.019.
- Zhong, S., and W. Leng (2006), Dynamics of mantle plumes and their implications for the heat budget and composition of the mantle, *Geochim. Cosmochim. Acta*, *70*(18), SA749, doi:10.1016/j.gca.2006.06.1351.
- Zhou, Y., F. A. Dahlen, G. Nolet, and G. Laske (2005), Finite-frequency effects in global surface-wave tomography, *Geophys. J. Int.*, *163*, 1087–1111, doi:10.1111/j.1365-246X.2005.02780.x.